Magnetic resonance on $LiCuVO_4$

Ch. Kegler[1], N. Büttgen[1,a], H.-A. Krug von Nidda[1], A. Krimmel[1], L. Svistov[1], B.I. Kochelaev[1], A. Loidl[1], A. Prokofiev[2], and W. Aßmus[2]

[1] Experimentalphysik V, Elektronische Korrelationen und Magnetismus, Institut für Physik, Universität Augsburg, 86135 Augsburg, Germany
[2] Physikalisches Institut, Johann-Wolfgang-Goethe-Universität, 60054 Frankfurt, Germany

Abstract. EPR and ^{7}Li NMR measurements were performed in the distorted inverse spinel $V(LiCu)O_4$ down to 1.5 K. Anisotropy effects on magnetic resonance spectra due to the Jahn-Teller distortion of the oxygen octahedra surrounding the copper ions are discussed. The estimation of the spin-spin interactions deduced from the EPR-relaxation rate ΔH reveals a situation comparable to the prototypical one-dimensional $S = 1/2$ Heisenberg antiferromagnet $CuGeO_3$. Approaching three-dimensional antiferromagnetic order ($T_N \approx 2$ K) from above, both magnetic relaxation rates, ΔH_{EPR} and $^7(1/T_1)$, respectively, exhibit nearly the same critical divergence reminding to the onset of three-dimensional order in two-dimensional layered systems.

PACS. 76.30.Fc Iron group (3d) ions and impurities (Ti-Cu) – 76.60.Es Relaxation effects – 75.30.-m Intrinsic properties of magnetically ordered materials

1 Introduction

Lithium-copper-vanadate crystallizes in an orthorhombically distorted inverse spinel structure (AB_2O_4), in which the non-magnetic V^{5+} ions occupy the tetrahedral A-sites, whereas Li^+ and Cu^{2+} are arranged in an ordered way on the octahedral B-sites [1]. To indicate this inverse site occupancy, in the following the chemical formula $V(LiCu)O_4$ will be used. The octahedral sublattice displays the same superstructure as magnetite [2] and the edge sharing Cu and Li octahedra form independent chains along [010] and [100]. $V(LiCu)O_4$ thus is characterized by subsequent planes of Li and Cu rods ordered along [100] and [010], respectively and forming stacks along the c direction [3], a concept of rod packing that has been proposed by O'Keeffe and Andersson [4]. For a detailed drawing of the crystal structure we refer to Lafontaine *et al.* [3]. The orthorhombic symmetry follows from a cooperative Jahn-Teller distortion of the single hole in the e_g crystal-field level of the electronic configuration of the Cu^{2+} ions. Hence, in this system the only unpaired spin density is within the a, b-plane and is of $d_{x^2-y^2}$ symmetry.

The susceptibility has been measured several times [1,5–7]. At high temperatures a Curie-Weiss behavior with a Curie-Weiss temperature Θ of approximately -15 K has been reported with Θ slightly depending on the temperature range where it has been analyzed, and a paramagnetic moment due to a spin $S = 1/2$ and a g-value of the order 2.2, typical for Cu^{2+} in an octahedral environment. On decreasing temperature the susceptibility passes through a broad maximum close to 28 K. A subsequent strong increase towards lower temperatures and a peak-like anomaly around $T = 3$ K signals long-range magnetic order.

The interpretation of these results however, remains controversial. While Blasse [1] and González *et al.* [5] claim two-dimensional antiferromagnetic behavior with the onset of long-range three-dimensional antiferromagnetism at low temperatures, a detailed analysis by Yamaguchi *et al.* [6] reveals rather an one-dimensional character of the magnetic subsystem at elevated temperatures. They were able to fit the susceptibility and the heat capacity using a $S = 1/2$ one-dimensional Heisenberg antiferromagnet (AFM). They claim that the transition at 2.4 K indicates a transition into two-dimensional magnetic behavior. These very different interpretations result from the still unknown importance of the different exchange paths within the Cu chains (intrachain interaction) and in between neighboring copper chains (interchain interaction). Within the Cu chains there is a Cu-O-Cu 90° exchange, which according to the Kanamori-Goodenough rules should be predominantly ferromagnetic (FM), but becomes AFM for slight deviations of the bridge angle from 90°. Moreover, there exists a direct AFM exchange between Cu-Cu which should be relatively weak due to the large distance between neighboring Cu ions. The Cu-Cu distance r amounts 2.8 Å within the chains. Within the planes there exists a long-range superexchange between

[a] e-mail: n.buettgen@physik.uni-augsburg.de

different chains *via* Cu-O-V-O-Cu path which should be predominantly antiferromagnetic. There is only marginal coupling of the copper ions between different stacks.

^{7}Li and ^{51}V nuclear magnetic resonance (NMR) experiments were reported in the temperature range $77 < T < 413$ K by Saji [8]. For ^{7}Li spectra, quadrupolar satellites with a quadrupolar frequency $\nu_Q = 48$ kHz appeared in addition to the central resonance line. The strong positive isotropic Knight shift of the ^{51}V line was taken as experimental evidence for two-dimensional magnetism [8].

In this work we report on magnetic susceptibility, electron paramagnetic resonance (EPR) at X-band frequencies and ^{7}Li NMR results on polycrystalline samples. The main focus was to investigate the nature of low-dimensional magnetic behavior and the 3 K-phase transition in more detail.

2 Experimental details, results and discussion

2.1 Sample preparation and characterization

$V(LiCu)O_4$ powder samples were prepared by solid-state synthesis from a stoichiometric mixture of lithium carbonate Li_2CO_3 (99.9%), V_2O_5 (99.5%) and CuO. The powdered mixture was pressed in pellets and annealed at 550 °C during several days with intermediate grindings and pressings.

To characterize our samples, powder X-ray diffraction measurements have been performed at room temperature with an incident wavelength of 1.54 Å (Cu$K_{\alpha 1}$ radiation). All diffraction data were analyzed by standard Rietveld refinement employing the FULLPROF program [9]. The X-ray diffraction pattern and the results of the structural refinement are shown in Figure 1. Assuming the orthorhombically distorted spinel structure described by space group Imma, all reflections can be accounted for resulting in lattice constants of $a = 5.6599(3)$ Å, $b = 5.8108(3)$ Å and $c = 8.7595(4)$ Å in excellent agreement with the results reported in literature [3]. However, the corresponding reliability factors of the structural refinement of ≈ 0.19 are insufficient. The reason becomes clear when looking in detail at the diffractogram. Five reflections exhibit significant peak splittings corresponding to a lowering of the symmetry from orthorhombic to (at least) monoclinic. To illustrate this splitting, the (2 0 0) reflection is shown in the inset of Figure 1. Some further peaks display an unusual peak shape, in particular a plateau-like maximum which can be attributed to a peak splitting. It should be noted that the Cagliotti resolution parameters have been determined by measuring a Si standard.

Significant disorder between Cu^{2+} and Li^{+} ions which occupy the crystallographic (4*d*) and (4*a*) sites, respectively, could not be observed. The crystallographic (4*d*) and (4*a*) sites within space group Imma become equivalent in the undistorted cubic spinel structure described by space group Fd3m. Therefore, a statistical distribution of Li and Cu would lift the orthorhombic distortion. Indeed, this holds true for the homologue compounds $V(CoLi)O_4$ and $V(NiLi)O_4$, where complete disorder between Li/Co or Li/Ni ions, respectively, leads to an undistorted cubic spinel structure [5].

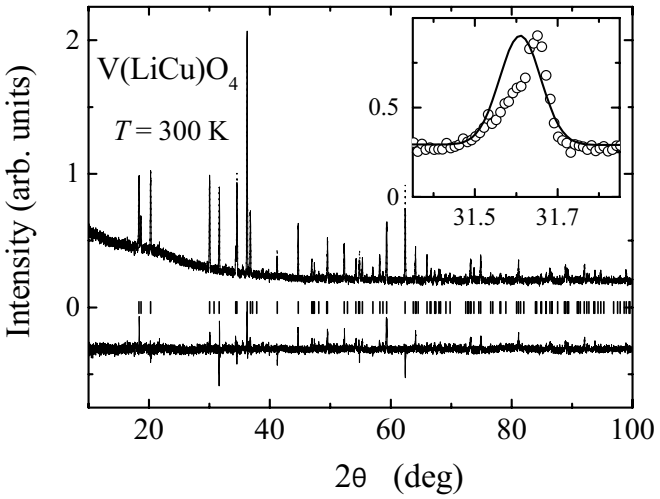

Fig. 1. X-ray diffraction pattern of $V(LiCu)O_4$ at room temperature. Full and dotted line correspond to observed and calculated intensities within space group Imma. In the lower part, the calculated peak positions (vertical bars) and the difference between calculated and observed intensities are shown. The inset shows the (2 0 0) reflection on an expanded scale, evidencing a possible peak splitting due to a lower symmetry than orthorhombic.

The crystallographic structure of reference [3] is an approximate description of the unit cell of $V(LiCu)O_4$, since the peak splitting is very weak and can only be observed in experiments with high resolution [10]. Furthermore, a slight sample dependence of the lattice distortions (depending for example on the exact oxygen stoichiometry) cannot be ruled out completely.

2.2 Results and discussion

2.2.1 SQUID magnetization

The temperature dependence $1.8 < T < 400$ K of the magnetization was measured in a commercial SQUID magnetometer (Quantum Design) at applied fields of 1000 Oe. Results are shown in Figure 2. At high temperatures the inverse susceptibility follows a linear behavior $\chi^{-1} \propto T - \Theta$ due to an antiferromagnetic Curie-Weiss law with $\Theta = -15$ K. The paramagnetic moment determined from the slope of the inverse susceptibility is due to one spin $S = 1/2$ per Cu atom with a g value of 2.15. Below 100 K, the susceptibility deviates from Curie-Weiss law exhibiting a pronounced maximum around $T_{\max} \approx 28$ K, which was interpreted controversially [6] as fingerprint of a one-dimensional Heisenberg antiferromagnet [11] or of two-dimensional antiferromagnetism [12]. Finally, a second peak at $T_N = 2.3$ K indicates the transition to antiferromagnetic order which is about 1.5 degree lower than

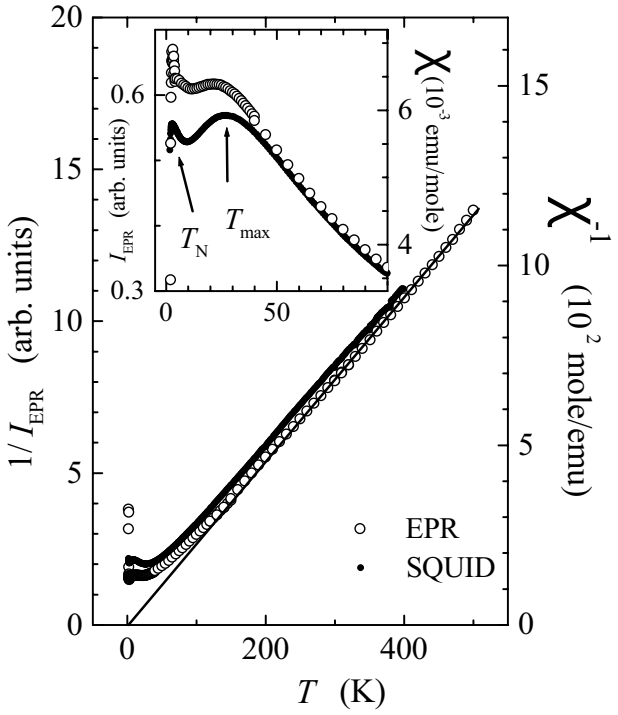

Fig. 2. Temperature dependence of the inverse EPR intensity $1/I_{\mathrm{EPR}}$ (open symbols) and the inverse static susceptibility $1/\chi$ (solid symbols). Inset: EPR-intensity and static susceptibility at temperatures $0 < T < 100$ K.

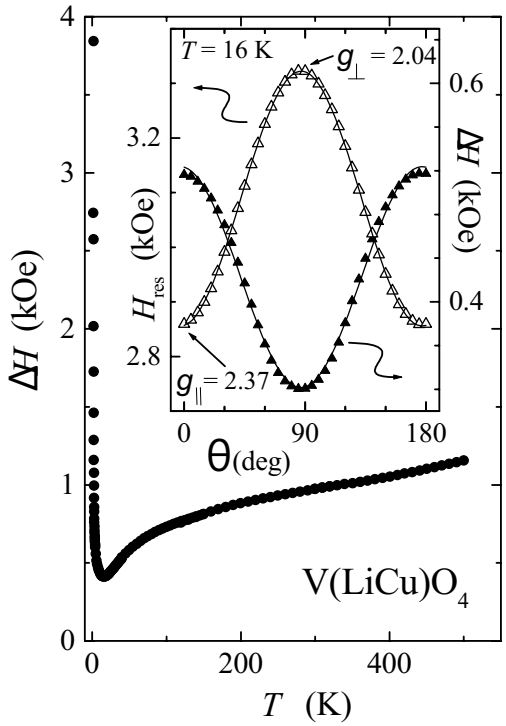

Fig. 3. Temperature dependence of the EPR linewidth $\Delta H(T)$ for $V(LiCu)O_4$ for powder without orientation. Inset: Angular dependence of resonance field (open symbols) and linewidth (solid symbols) for oriented powder. θ denotes the angle between the crystallographic c axis and the magnetic field H.

reported by Vasil'ev [7]. In addition, we compared field-cooled and zero-field-cooled magnetization within the low-temperature regime to exclude spin-glass behavior as the origin of the anomalies at T_{max} and T_{N}, respectively. Field dependent magnetization measurement do not give any evidence for spontaneous magnetization below T_{N} underlining the antiferromagnetic character of the ordered state.

2.2.2 EPR

The EPR experiments have been performed at a Bruker ELEXSYS E500-CW spectrometer at X-band frequencies (9.4 GHz) equipped with continuous gas-flow cryostats for He (Oxford Instruments) and N_2 (Bruker) in the temperature range between 4.2 and 500 K. For temperatures down to 1.7 K we used a cold-finger ^{4}He-bath cryostat. The powdered polycrystals were filled in quartz tubes, and fixed in paraffin for measurements below room temperature. For angular dependent measurements at low temperatures, the powder embedded in paraffin was partially oriented by first melting the paraffin and then cooling the whole sample within a magnetic field of 17 kOe: As the Jahn-Teller effect induces a uniaxial elongation along [001] direction of the oxygen octahedra surrounding the Cu^{2+}-ions [3], the magnetic susceptibility is assumed to be anisotropic with respect to the c axis due to symmetry reasons. Hence, the nearly single crystalline powder grains presumably align with the c axis parallel to the external field.

EPR detects the power absorbed by the paramagnetic sample from a transverse magnetic microwave field as a function of the static magnetic field H. The EPR spectra in $V(LiCu)O_4$ consist of a single exchange-narrowed resonance, which is nicely fitted by a Lorentzian line. The integrated EPR intensity I_{EPR} is comparable to the static susceptibility χ obtained from SQUID measurements as illustrated in Figure 2. At temperatures $T > 100$ K, both follow a Curie-Weiss law $\chi^{-1} \propto T - \Theta$. But, in the case of the EPR intensity the extrapolation yields a slightly different Curie-Weiss temperature $\Theta_{\mathrm{EPR}} \approx 0$ compared to the SQUID result $\Theta_{\mathrm{SQUID}} \approx -15$ K. At lower temperatures, the EPR intensity also deviates from the Curie-Weiss law and develops a maximum near $T_{\mathrm{max}} = 25$ K. Below 2.3 K where the static susceptibility gradually decreases, the EPR signal rapidly vanishes due to the opening of an antiferromagnetic excitation gap.

Figure 3 shows the temperature dependence of the resonance linewidth ΔH deduced from spectra of randomly oriented powder up to 500 K, since the orientation of the grains cannot be fixed in liquid paraffin above room temperature. At higher temperatures $T > 500$ K the sample changes its properties irreversibly due to some annealing process in the nitrogen atmosphere. Starting at its minimum value $\Delta H_{\mathrm{min}} \approx 400$ Oe at $T = 16$ K, the linewidth increases monotonously on increasing temperature. Below $T = 16$ K the resonance line strongly broadens approaching the magnetic order at 2.3 K. For the oriented powder, the angular dependence of the resonance field H_{res} and linewidth ΔH are sketched in the inset of Figure 3 for

the temperature with the minimum linewidth $T = 16$ K, because the smaller the linewidth the better the accuracy of the determined resonance field $H_{\rm res}$. Both, resonance field and linewidth follow a $\cos^2\theta$ law indicated by solid lines. The maximum linewidth coincides with the maximum of the g tensor. The experimental values $g_\parallel \approx 2.37$ and $g_\perp \approx 2.04$ are typical for Cu^{2+} in octahedral coordination like for example in $CuGeO_3$ [13,14]. With increasing temperature the mean value $g = (g_\parallel + 2g_\perp)/3 \approx 2.15$ remains constant in excellent agreement with the magnetization data, whereas the g anisotropy seems to decrease slightly and deviates from the $\cos^2\theta$ law. However, the ratio $\Delta H_\parallel/\Delta H_\perp \approx 1.6$ remains nearly unchanged or even increases slightly, indicating that the effect on the g value may be due to missorientation, which becomes more and more effective with increasing linewidth.

To understand the origin of the observed linewidth, we have to estimate the relaxation contributions of the relevant spin-spin interactions, as there are dipole-dipole (DD), anisotropic exchange (AE), and antisymmetric Dzyaloshinsky-Moriya (DM) interaction. In the case of strong exchange narrowing, the magnitude of these contributions can easily be calculated in the high-temperature limit ($T \gg J/k_{\rm B}$) following Pilawa [14] and Yamada [13]:

Dipole-dipole interaction:

$$\Delta H_{\rm DD}({\rm kOe}) = \frac{3g^3\mu_B^3 S(S+1)}{k_{\rm B}|J|r^6} = 13\frac{g^3}{|J({\rm K})|r^6({\rm \AA})}\,. \quad (1)$$

Anisotropic exchange:

$$\Delta H_{\rm AE}({\rm kOe}) = \frac{3S(S+1)A^2}{2g\mu_{\rm B}k_{\rm B}|J|} = 17\left(\frac{\Delta g}{g}\right)^4\frac{|J({\rm K})|}{g}\,. \quad (2)$$

Dzyaloshinsky-Moriya interaction:

$$\Delta H_{\rm DM}({\rm kOe}) = \frac{S(S+1)}{3g\mu_{\rm B}}\frac{|\mathbf{d}_{\rm DM}|^2}{k_{\rm B}|J|} = 3.7\left(\frac{\Delta g}{g}\right)^2\frac{|J({\rm K})|}{g} \quad (3)$$

where J denotes the isotropic Heisenberg exchange measured in kelvin and A the anisotropic exchange which was estimated *via* the anisotropy of the g factor ($\Delta g \approx 0.3$ see inset Fig. 3) as $A \approx (\Delta g/g)^2 k_{\rm B}|J|$. The absolute value of the DM vector $\mathbf{d}_{\rm DM}$ was roughly approximated by $|\mathbf{d}_{\rm DM}| = (\Delta g/g)\, k_{\rm B}|J|$ [13]. To obtain the final expressions we inserted spin $S = 1/2$ and the Bohr magneton $\mu_{\rm B}$ and the Boltzmann constant $k_{\rm B}$ in *cgs* units. The copper-copper distance $r \approx 2.8$ Å is half of the lattice parameter b. In order to estimate the magnitude of the experimentally observed linewidth we need reliable values for the exchange coupling J. Assuming a dominant one- or two-dimensional AFM coupling as proposed by different authors [6,8], the value of $J({\rm K}) \approx -28$ K is approximately given by the temperature of the susceptibility maximum. This yields $\Delta H_{\rm DD} = 7.5$ Oe, $\Delta H_{\rm AE} \approx 120$ Oe, and $\Delta H_{\rm DM} \approx 1.16$ kOe. Hence, we find that the dipole-dipole interaction is negligible, whereas the anisotropic exchange and DM interaction dominantly account for the linewidth. Like in the case of $CuGeO_3$, the latter contribution (DM) can not be constructed from the next-neighbors interactions, because the DM vectors of neighboring Cu-O-Cu bridges cancel each other. Hence, the relevance of the DM interaction remains an open question in $V(LiCu)O_4$ and needs careful theoretical investigations. On the other hand, the intermediate value of the anisotropic exchange does not seem to account entirely for the observed linewidth (Fig. 3). Additional contributions to the linewidth may arise from spin-phonon interactions.

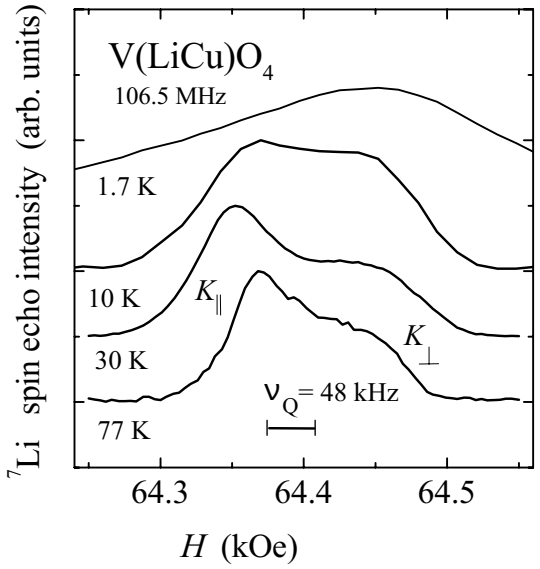

Fig. 4. ^{7}Li NMR field-swept spectra for temperatures $1.7 < T < 77$ K. The bar indicates a quadrupolar frequency $\nu_{\rm Q}$ taken from reference [8].

2.2.3 NMR

The NMR measurements have been carried out with a phase-coherent pulse spectrometer probing the ^{7}Li nuclei residing at the octahedral B-sites (spin $I = 3/2$, gyromagnetic ratio $\gamma = 16.546$ MHz/T). Spectra were obtained using field sweeps $64.25 < H_0 < 64.55$ kOe at a constant radio frequency $\omega_0/2\pi = 106.5$ MHz. The spectra were collected using a conventional 20 μs-$\tau_{\rm D}$-40 μs spin-echo sequence ($\tau_{\rm D} = 100$ μs).

Figure 4 shows ^{7}Li spectra for several temperatures at a radio frequency of $\omega_0/2\pi = 106.5$ MHz. At lowest temperature $T = 1.7$ K the spectrum exhibits strong broadening and resonance shift to higher fields ($\delta H/H_{\rm res} \approx 0.1\%$) due to a wide inhomogeneous distribution of transferred hyperfine fields as it is indicative for three dimensional magnetic ordering. At elevated temperatures one observes that the lineshape is affected by drastic magnetic anisotropy and electric quadrupolar interaction as it has been reported by Saji [8]. A corresponding quadrupolar frequency $\nu_{\rm Q} = 48$ kHz (indicated as a bar in Fig. 4) was deduced from a powder pattern with nicely resolved first-order satellite transitions at a radio frequency $\omega_0/2\pi = 14.892$ MHz [8]. In our case at about seven times higher

Larmor frequency and magnetic fields, strong magnetic broadening covers this first-order quadrupolar splitting, which in turn is field independent. A parallel and perpendicular contribution ($K_\parallel$ and $K_\perp$, respectively) of the magnetic anisotropy shift can be distinguished as indicated in Figure 4 at $T = 77$ K. It may be surprising that we identify the stronger peak with $K_\parallel$ in contrast to usual powder patterns exhibiting a dominating perpendicular resonance contribution $K_\perp$ for geometrical reasons.

However, since we used unfixed powder, we can attribute this inverse intensity ratio to partial orientation of the microcrystalline grains. This is corroborated, if we look closer to the low-frequency spectrum from Saji [8] at the same temperature: An anisotropic Knight shift of about 80 Oe, found in our high-field experiment, can easily be transferred to the spectrum at $\omega_0/2\pi = 14.892$ MHz in the same ratio as the ratio of the corresponding radio frequencies. Due to nicely resolved first-order satellite lines, the spacing between corresponding satellites is clearly attributed to both orientations: The quadrupolar splitting is two times larger for parallel satellite lines with tiny intensity compared to the perpendicular oriented ones [15]. Without anisotropic Knight shift the centers of both satellite pairs should coincide. However, the parallel pattern is shifted by an amount of ≈ 10 Oe to lower fields with respect to the perpendicular pattern. This field shift satisfactorily equals the expected anisotropic Knight shift. Note that the parallel oriented pattern is found at the low field side of the spectrum.

We determined the spin-lattice relaxation rate $1/T_1$ from the inversion recovery of the spin-echo intensity irradiating the center of the anisotropic powder pattern. The recovery of the nuclear magnetization $M(\tau)$ was best fitted to a stretched-exponential relaxation behavior $M(\tau) \propto \exp[-(\tau/T_1)^\lambda]$ within a pulse-separation interval of four decades in time. This stretched-exponential behavior of the magnetization recovery does not signal disorder effects, but obviously is a good approximation of the complex relaxation due to the mixing of multiexponential recoveries of each orientation, since the relaxation of signals from parallel and perpendicular irradiation are influenced by different quadrupolar splittings. It becomes even more obvious as the stretching exponent $\lambda \approx 0.5$ remains constant for all temperatures. The temperature dependence of the spin-lattice relaxation rate $1/T_1$ is presented in Figure 5 for temperatures $1.5 < T < 80$ K in an external magnetic field of 64.4 kOe. For temperatures $T > 20$ K the spin-lattice relaxation rate $1/T_1$ increases linearly up to about 50 K and then approximately saturates for higher temperatures. For low temperatures $T < 10$ K the divergence of $1/T_1(T)$ can be fitted with a critical exponent $\beta = -0.66(2)$ and $T_N = 1.30(1)$ K. This temperature corresponds to a peak in the experimental data that indicates critical fluctuations accompanied by a magnetic transition.

It is interesting to note that the EPR linewidth ΔH exhibits a comparable power law with $\beta = -0.55(3)$ in the same temperature range as displayed in the inset of Figure 5 with no additional fitting parameter due to any

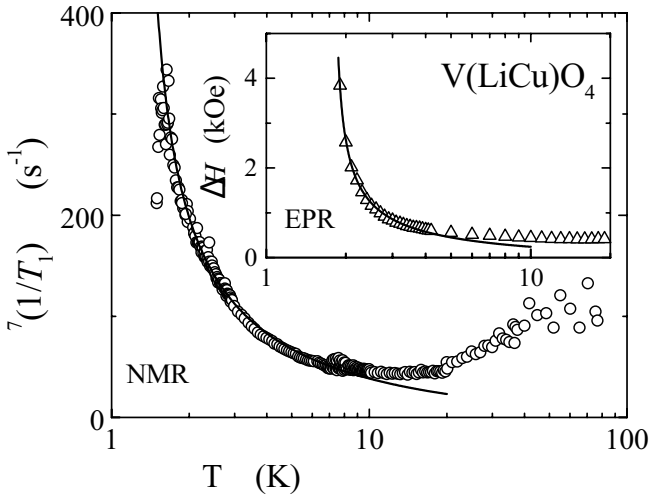

Fig. 5. NMR $1/T_1$ and EPR linewidth ΔH *vs.* log$T$. The solid lines are fits $1/T_1 \propto (T - T_N)^\beta$. NMR: $T_N = 1.30(1)$ K, $\beta = -0.66(2)$; EPR: $T_N = 1.81(1)$ K, $\beta = -0.55(3)$, respectively. The slight difference in T_N is in principle agreement with the field dependent phase-transition temperatures proposed in the phase diagram by Vasil'ev [7].

residual linewidth ΔH_0 being introduced. Theoretical predictions concerning the critical exponent β of $\Delta H(T)$ in two- or three-dimensional AFM yield about $-2.6 \cdots -3.3$ and $-1.7 \cdots -1.8$, respectively [16]. However, the experimental findings reported in the same review give smaller values of about $-0.5 \cdots -0.7$ in the temperature regime close to T_N in similar layer-type compounds with interplanar coupled AFM fluctuations. Possibly, the striking similarity to the ^{7}Li nuclear spin-lattice relaxation rate $1/T_1(T)$ stems from this interplanar coupling probed at the interplanar Li site.

3 Conclusion

To summarize, we presented synoptic EPR and ^{7}Li NMR investigations in polycrystalline V(LiCu)O$_4$ down to 1.5 K. This compound is characterized by a well defined sublattice order of Li and Cu ions sharing every two corners of a tetrahedron within the inverse spinel structure forming chains in a and b directions, respectively. This rules out geometrical magnetic frustration which is usually effective in compounds with magnetic ions at the corners of a tetrahedron [17]. The cooperative Jahn-Teller distortion of oxygen octahedra surrounding the Cu^{2+} ions causes pronounced anisotropy effects on the magnetic resonance spectra: Concerning the NMR experiment a strong anisotropic Knight shift was found to be responsible for an observed double-peak structure masking the quadrupolar splitting reported for low-field measurements [8] and yielding a complex nuclear magnetization recovery which was best fitted by a stretched exponential form.

The EPR, probing the dynamic susceptibility of the Cu^{2+} spins, reveals a temperature dependent intensity in reasonable agreement with the static susceptibility $\chi(T)$.

Low dimensional magnetic behavior is corroborated by the maximum in the temperature dependence of the static susceptibility as well as in the EPR intensity at $T \approx 28$ K. To explain the observed EPR linewidth, the estimation of the different relaxation mechanisms turned out an appreciable contribution due to DM and anisotropic exchange interactions. Nevertheless, the microscopic explanation of the DM interaction in $V(LiCu)O_4$ needs further investigation on single crystalline material accompanied by theoretical calculations.

Below $T = 10$ K, both relaxation rates, $\Delta H_{\rm EPR}$ and $^7(1/T_1)$, respectively, exhibit critical fluctuations which we ascribe to onset of three-dimensional magnetic order *via* interplanar coupling. Based on these results, we conclude that $V(LiCu)O_4$ reveals a scenario of subsequent magnetic regimes ranging from one-dimensional ($T > 30$ K) to three-dimensional AFM order below $T < 2$ K. In the intermediate temperature range there are hints for two-dimensional magnetism due to the critical increase of the temperature dependent relaxation rates of both EPR and NMR experiments with small critical exponent.

We kindly acknowledge M. Müller, A. Pimenova and D. Vieweg for SQUID and X-ray characterization. This work was supported by the BMBF under contract No. 13N6917 (EKM) and partly by the Deutsche Forschungsgemeinschaft (DFG) *via* the Sonderforschungsbereich 484 and DFG-project No. 436 RUS 113/566/0. B.I. Kochelaev was partially supported by RFFI grant No. 00-02-04015.

References

1. G. Blasse, J. Phys. Chem. Solids **27**, 612 (1965).
2. E.J.W. Verwey, Nature **144**, 327 (1939); E.J.W. Verwey, P.W. Haayman, Physica **8**, 979 (1941).
3. M.A. Lafontaine, M. Leblanc, G. Ferey, Acta Crys. C **45**, 1205 (1989).
4. M. O'Keeffe, S. Andersson, Acta Crys. A **33**, 914 (1977).
5. C. González, M. Gaitán, M.L. López, M.L. Veiga, R. Saez-Puche, C. Pico, J. Mat. Science **29**, 3458 (1994).
6. M. Yamaguchi, T. Furuta, M. Ishikawa, J. Phys. Soc. Jpn **65**, 2998 (1996).
7. A.N. Vasil'ev, JETP Lett. **69**, 879 (1999).
8. H. Saji, J. Phys. Soc. Jpn **33**, 671 (1972).
9. J. Rodriguez-Carvajal, Physica B **192**, 55 (1993).
10. Note that we used $CuK_{\alpha 1}$ radiation corresponding to $\lambda = 1.5409$ Å as compared to MoK_α radiation corresponding to $\lambda = 0.7107$ Å of reference [3]. Reference [5] concentrates on the Ni/Co homologue compounds and does not give any structural information on $V(LiCu)O_4$. According to González *et al.*, their X-ray diffraction measurements have also been performed employing $CuK_{\alpha 1}$ radiation, however with a four times larger angular step size.
11. J.C. Bonner, M.E. Fisher, Phys. Rev. **135**, A640 (1964).
12. M.E. Lines, J. Phys. Chem. Solids **31**, 101 (1970).
13. I. Yamada, M. Nishi, J. Akimitsu, J. Phys. Cond. Matt. **8**, 2625 (1996).
14. B. Pilawa, J. Phys. Cond. Matt. **9**, 3779 (1997).
15. W.H. Jones Jr., T.P. Graham, R.G. Barnes, Phys. Rev. **132**, 1898 (1961).
16. H. Benner, J.P. Boucher, in *Magnetic Properties of Layered Transition Metal Compounds*, edited by L.J. de Jongh (Kluwer Academic Publishers, 323, 1990), p. 368.
17. H. Kaps, M. Brando, W. Trinkl, N. Büttgen, A. Loidl, E.-W. Scheidt, M. Klemm, S. Horn, to be published.